

Published in final edited form as:

*Pharmacol Res Perspect.* 2014 October ; 2(5): e00061-. doi:10.1002/prp2.61.

## Moderate, chronic ethanol feeding exacerbates carbon-tetrachloride-induced hepatic fibrosis via hepatocyte-specific hypoxia inducible factor 1 $\alpha$

Sanjoy Roychowdhury<sup>1</sup>, Dian J. Chiang<sup>2</sup>, Megan R. McMullen<sup>1</sup>, and Laura E. Nagy<sup>1,2,3</sup>

<sup>1</sup>Center for Liver Disease Research, Department of Pathobiology, Cleveland Clinic, Cleveland, Ohio

<sup>2</sup>Department of Gastroenterology, Cleveland Clinic, Cleveland, Ohio

<sup>3</sup>Department of Molecular Medicine, Case Western Reserve University, Cleveland, Ohio

### Abstract

The hypoxia-sensing transcriptional factor HIF1 $\alpha$  is implicated in a variety of hepato-pathological conditions; however, the contribution of hepatocyte-derived HIF1 $\alpha$  during progression of alcoholic liver injury is still controversial. HIF1 $\alpha$  induces a variety of genes including those involved in apoptosis via p53 activation. Increased hepatocyte apoptosis is critical for progression of liver inflammation, stellate cell activation and fibrosis. Using hepatocyte-specific HIF1 $\alpha$ -deficient mice (HepHIF1 $\alpha$ -/-), here we investigated the contribution of HIF1 $\alpha$  to ethanol-induced hepatocyte apoptosis and its role in amplification of fibrosis after carbon tetrachloride (CCl<sub>4</sub>) exposure. Moderate ethanol feeding (11% of Kcal) induced accumulation of hypoxia-sensitive pimonidazole adducts and HIF1 $\alpha$  expression in the liver within 4 days of ethanol feeding. Chronic CCl<sub>4</sub> treatment increased M30-positive cells, a marker of hepatocyte apoptosis in pair-fed control mice. Concomitant ethanol feeding (11% of Kcal) amplified CCl<sub>4</sub>-induced hepatocyte apoptosis in livers of wild-type mice, associated with elevated p53<sup>K386</sup> acetylation, PUMA expression and Ly6c<sup>+</sup> cell infiltration. Subsequent to increased apoptosis, ethanol enhanced induction of pro-fibrotic markers including stellate cell activation, collagen 1 expression and extracellular matrix deposition, following CCl<sub>4</sub> exposure. Ethanol-induced exacerbation of hepatocyte apoptosis, p53<sup>K386</sup> acetylation and PUMA expression following CCl<sub>4</sub> exposure was attenuated in livers of HepHIF1 $\alpha$ -/- mice. This protection was also associated with a reduction in Ly6c<sup>+</sup> cell infiltration and decreased fibrosis in livers of HepHIF1 $\alpha$ -/- mice. In summary, these results indicate that moderate ethanol exposure leads to hypoxia/HIF1 $\alpha$ -mediated signaling in hepatocytes and induction of p53-dependent apoptosis of hepatocytes, resulting in increased hepatic fibrosis during chronic CCl<sub>4</sub> exposure.

Address correspondence to: Laura E. Nagy, Cleveland Clinic Foundation, Lerner Research Institute/NE40, 9500 Euclid Ave, Cleveland OH 44195, Phone 216-444-4120, Fax 216-636-1493, len2@po.cwru.edu.

#### Authorship contribution:

Participated in research design: Roychowdhury, Chiang, McMullen and Nagy

Conducted experiments: Roychowdhury, Chiang, McMullen

Performed data analysis: Roychowdhury, Chiang

Writing of the manuscript: Roychowdhury and Nagy

*Conflicts of interest:* The Authors who have taken part in this study declared that they do not have anything to disclose regarding funding or conflict of interest with respect to this manuscript.

## Keywords

Hypoxia; hypoxia inducible factor 1 $\alpha$ ; ethanol; carbon tetrachloride; liver; fibrosis; apoptosis; inflammation; collagen; hepatic stellate cells

---

## Introduction

The initiation and progression of fibrosis in the liver is tightly regulated by multiple pathways involving different hepatic and immune cell types (Bataller and Brenner, 2005; Bataller et al., 2011). While macrophages and hepatic stellate cells (HSC) are considered to be the primary cell types mediating the inflammatory and pro-fibrotic responses to liver injury (Ramachandran and Iredale, 2012a; Ramachandran and Iredale, 2012b), recent evidence indicates that hepatocytes also contribute to development of liver fibrosis (Copple et al., 2009). For example, apoptosis of hepatocytes is a critical factor for progression of liver fibrosis (Canbay et al., 2004). Phagocytosis of apoptotic hepatocytes by macrophages and HSCs activates these cells, resulting in the induction of pro-inflammatory/ pro-fibrogenic responses in the liver (Canbay et al., 2004). Further, hepatocyte-specific deletion of transcription factors, including Snail, a hypoxia-sensitive transcription factor (Rowe et al., 2011), and Smad 7, a regulator of TGF $\beta$  expression (Dooley et al., 2008), attenuate hepatic fibrosis, suggesting a role for hepatocyte-generated signals during activation of liver fibrosis. Taken together, studies such as these identify the hepatocyte as a critical player during the propagation of liver fibrosis.

Chronic alcohol consumption is a major risk factor for development of hepatic fibrosis (Bataller et al., 2011); however, the molecular mechanisms of alcohol-driven pro-fibrogenic responses in the liver are still not well understood. Understanding the pathophysiological mechanisms for alcohol's contribution to the development of hepatic fibrosis will aid in the development of pharmacological interventions to both prevent and reverse alcoholic liver disease.

Recent studies have identified several pathways by which ethanol can enhance fibrotic responses. For example, ethanol-induced hepatocyte apoptosis is associated with increased fibrogenesis [Roychowdhury, et al., 2012]. Furthermore, ethanol metabolism by hepatocytes likely contributes to the development of hepatic fibrosis. The impact of the by-products of alcohol metabolism, acetaldehyde and reactive oxygen species (ROS), has been well studied. Acetaldehyde and ROS activate HSC and induce fibrosis via transcriptional up-regulation of pro-fibrotic mediators, including transforming growth factor (TGF $\beta$ 1), and thus increase extracellular matrix deposition (Mormone et al., 2011). However, the role for hypoxia, another consequence of ethanol metabolism (Wang et al., 2013), in ethanol-driven amplification of liver fibrosis has not been well studied and is the focus of the current investigation.

Cellular responses to hypoxia are primarily mediated via stabilization of the hypoxia inducible factor 1 $\alpha$  (HIF1 $\alpha$ ), an oxygen-sensing transcription factor (Nath and Szabo, 2012). In response to hypoxia, HIF1 $\alpha$  translocates from cytosol to the nucleus and forms dimers with HIF1 $\beta$ , a nuclear protein, and subsequently triggers transcription of a variety of genes,

including the pro-inflammatory/fibrotic genes such as VEGF, iNOS and COX-2 (Hirota et al., 2009). Hepatocyte-specific HIF1 $\alpha$  is critical for a variety of liver pathologies including ischemia/reperfusion injury and drug-induced liver injury (Cursio et al., 2008; Wu et al., 2008; Nath and Szabo, 2012). Stabilization of HIF1 $\alpha$  in hepatocytes has also been implicated in the progression of liver fibrosis following bile duct ligation(BDL)-induced hepatic injury (Moon et al., 2009).

While it is clear that ethanol feeding induces localized hypoxia in the liver (Nishiyama et al., 2012; Chiang et al., 2013), the role of HIF1 $\alpha$  in different stages of alcoholic liver disease is still controversial and not well understood. For example, HIF1 $\alpha$  in hepatocytes has been reported to play both a protective (Nishiyama et al., 2012) and injurious (Nath and Szabo, 2012) role during ethanol-induced steatosis and inflammation in mouse models of *ad lib* ethanol feeding.

While these conflicting results on the role of HIF1 $\alpha$  in the early stages of ethanol-induced liver injury demand more detailed studies (Mehal, 2012), it is also critical to ascertain the role of HIF1 $\alpha$  in the association between chronic ethanol consumption and hepatic fibrosis. Making use of a novel model in which moderate ethanol exposure exacerbates CCl<sub>4</sub>-induced hepatic fibrosis, we recently identified hepatocyte apoptosis as a critical contributor to ethanol's ability to amplify CCl<sub>4</sub>-induced fibrosis (Roychowdhury et al., 2012). One potential pathway of ethanol-induced apoptosis in the context of CCl<sub>4</sub>-induced fibrosis is via HIF1 $\alpha$ -dependent pathways. HIF1 $\alpha$ -induced apoptotic cell death is largely p53-dependent (Greijer and van der Wall, 2004) and p53 is activated during progression of CCl<sub>4</sub>-induced liver fibrosis (Guo et al., 2013). Therefore, here we hypothesized that ethanol-driven hypoxia/HIF $\alpha$  activation induces p53 activation and apoptosis in hepatocytes, which subsequently leads to amplification of CCl<sub>4</sub>-induced pro-fibrotic responses in the liver. Making use of hepatocyte-specific HIF1 $\alpha$ -deficient mice, here we identified that moderate ethanol feeding in the context of CCl<sub>4</sub> exposure activated hypoxia/HIF1 $\alpha$ -mediated signaling in hepatocytes, leading to increased acetylation of p53 and hepatocyte apoptosis. These HIF1 $\alpha$ -dependent responses in hepatocytes were critical for the exacerbation of CCl<sub>4</sub>-induced pro-fibrotic responses following moderate ethanol exposure.

## Materials and methods

### Materials

Female C57BL/6J mice (10–12 weeks old) were purchased from Jackson Labs (Bar Harbor, Maine). Lieber-DeCarli high-fat ethanol and control diets were purchased from Dyets (Bethlehem, PA). Antibodies were from the following sources: anti-pimonidazole-adduct (Hypoxyprobe Inc., Burlington, MA), HIF1 $\alpha$  (Novus Biologicals, Littleton, CO), Collagen 1 (Southern Biotech, Birmingham, AL),  $\alpha$ -smooth muscle actin (Sigma-Aldrich, St. Louis, MO), CYP2E1 (abcam, Eugene, OR), HSC70 (Santa Cruz Biotechnology, Inc, Santa Cruz, CA), Acetylated p53<sup>K386</sup> (abcam, Eugene, OR), PUMA (Millipore, Billerica, MA) and M30/anti-cytokeratin 18 fragments (Roche, Mannheim, Germany). Ly6c-FITC antibody was obtained from AbD Serotec (Raleigh, NC). Direct red was obtained from Sigma-Aldrich (St. Louis, MO). Alexa Fluor 488 and 568-conjugated secondary antibodies were obtained from Invitrogen (Carlsbad, CA).

### Generation of hepatocyte-specific HIF1 $\alpha$ -deficient mice

A homozygous colony of hepatocyte-specific HIF1 $\alpha$ -deficient (HepHIF1 $\alpha$ <sup>-/-</sup>) mice on a C57BL/6 background (Ding et al., 2004) was established at the Cleveland Clinic by serial crossing of HIF1 $\alpha$ <sup>fl/fl</sup> (B6.129-HIF1 $\alpha$ <sup>tm3Rsj/J</sup>) mice with Alb-Cre (B6.Cg-Tg(Alb-cre)21Mgn/J) mice that express the Cre-recombinase under the albumin promoter. Both the parental strains were obtained from Jackson Labs (Bar Harbor, Maine). Mice were genotyped after each generation and checked for hepatocyte-specific conditional deletion of HIF1 $\alpha$  allele. Genomic DNA was extracted by digesting mouse tail tissue in proteinase-K solution (1mg/ml, Roche, Mannheim, Germany) at 50 °C overnight. Hair and undigested debris were removed by centrifugation and DNA was collected via ethanol precipitation. Real-time polymerase chain reaction analysis was done using Bullseye EvaGreen SYBR qPCR reagent (MidSci, St. Louis, MO) on a Chromo4 Cyclor (MJ Research/Bio-Rad, Hercules, CA) using primer sequences as follows Hif1 $\alpha$  forward primer CGT GTG AGA AAA CTT CTG GAT G; reverse primer AAA AGT ATT GTG TTG GGG CAG T; cre forward primer TGA TGG ACA TGT TCA GGG ATC; reverse primer CAG CCA CCA GCT TGC ATG A. PCR conditions were detailed as follows: 95 °C for 5 min, 95 °C for 30 sec, 58 °C for 5 30 sec, 72 °C for 30 sec followed by 35 cycles of 95 °C for 30 sec, 72 °C for 5 min and 4 °C on hold. PCR products were resolved on a 2% agarose gel with ethidium bromide; Hif1 $\alpha$  primers yield 3 potential fragments, a 565 bp fragment for a WT animal, 565 and 615 bp fragments for a heterozygote, and 615bp for a KO animal. Cre primers yielded a 865 bp fragment. Primer concentration was used as 0.5  $\mu$ M per primer and dNTP concentration used was 0.2 mM.

### Mouse models of moderate ethanol and carbon tetrachloride

In order to study the interaction between ethanol and CCl<sub>4</sub>-induced liver fibrosis, mice were subjected to chronic CCl<sub>4</sub>-treatment combined with moderate ethanol (11% of Kcal) feeding. The concentration and duration of ethanol feeding used in this model does not induce expression of cytochrome P450 monooxygenase (CYP2E1), a key enzyme for ethanol metabolism, as well as bioactivation of CCl<sub>4</sub> (Roychowdhury et al., 2012; Chiang et al., 2013) (Supplemental Figure 2). The combination of moderate ethanol with CCl<sub>4</sub> results in an exacerbation of hepatic fibrosis, characterized by increased activation of HSC and accumulation of extracellular matrix (Roychowdhury et al., 2012; Chiang et al., 2013).

Female mice were housed in shoe-box cages (2 animals/cage) with microisolator lids. Standard microisolator handling procedures were used throughout the study. Mice were randomized into ethanol-fed and pair-fed groups and then adapted to control liquid diet for 2 days. The ethanol-fed group was then allowed free access to an ethanol containing diet with 1% (vol/vol) ethanol for 2 days, then 2% (vol/vol) ethanol for the remainder of the study. The 2% diet provided 11% of calories as ethanol. After 4 days of ethanol feeding, mice were injected with 0.25  $\mu$ l/g CCl<sub>4</sub> (SIGMA, St. Louis, MO, Cat. No. 270652), followed 0.50  $\mu$ l/g CCl<sub>4</sub> 3 days later and then administered 1 $\mu$ l/g body weight of CCl<sub>4</sub> (intra-peritoneally twice a week) using 100  $\mu$ l Hamilton syringes fitted with 26G 5/8 inch needles for 5 weeks. Mice continued on either the control or ethanol diet (11% of calories) during the CCl<sub>4</sub> exposure period.

Seventy two hours after the last CCl<sub>4</sub> injection, mice were anesthetized, blood samples taken into non-heparinized syringes from the posterior vena cava and livers excised. Portions of each liver were then either fixed in formalin or frozen in optimal cutting temperature (OCT) compound (Sakura Finetek U.S.A., Inc., Torrance CA) for histology, frozen in RNAlater (Qiagen, Valencia, CA) or flash frozen in liquid nitrogen and stored at -80 °C until further analysis. Blood was transferred to EDTA-containing tubes for the isolation of plasma. Plasma was then stored at -80°C.

All procedures using animals were approved by the Cleveland Clinic Institutional Animal Care and Use Committee.

In order to confirm that each of the parental strains had a similar response to EtOH/CCl<sub>4</sub> exposure, Sirius red staining was assessed as a measure of fibrosis. C57BL/6 mice as well as the parental HIF1 $\alpha$ <sup>fl/fl</sup> and Alb-cre mice exhibited comparable increases in ethanol-induced Sirius red staining following chronic CCl<sub>4</sub> exposure (see Figure 4). Therefore, C57BL/6 mice were used as controls for all other studies.

### Detection of hypoxia

After 4 days of ethanol feeding mice were injected with the hypoxia-sensing drug, pimonidazole, 1 hour before euthanasia (Chiang et al., 2013). Samples were collected as detailed above.

### Western blot analysis

Frozen liver tissue (0.5 –1.0 g) was homogenized in lysis buffer (10 ml/ g tissue) containing 50 mM Tris-HCl, pH7.4, 1% NP-40, 0.25% Na-deoxycholate, 150 mM NaCl, 1 mM EDTA with added protease inhibitors Complete™ (Roche Diagnostics, Mannheim, Germany), 17.5 µg/ml aprotinin, 5µg/ml bestatin, 10 µg/ml leupeptin, 1 mg/ml bacitracin, and 20 µg/ml E64 and phosphatase inhibitors (1 mM vanadate and 10 mM Na pyrophosphate) using 15 strokes in a glass on glass homogenizer (loose pestle). After 15 min on ice, samples were centrifuged at 16,000 × g for 15 min to remove insoluble material followed by protein concentration measurement using the BCA assay (Pritchard et al., 2007). Liver lysates were then normalized and prepared in Laemmli buffer and boiled for 5 min. Samples were separated by 10% SDS-polyacrylamide gel electrophoresis and transferred to membranes for Western blotting. Membranes were incubated with rabbit anti-CYP2E1-antibody (Research Diagnostics, Inc., Flanders, NJ, 1: 200 dilution) overnight at 4 °C, then washed and incubated for 1 h in anti-rabbit secondary antibody (1: 25000 dilution) coupled to horseradish peroxidase. Immunoreactive proteins were detected using enhanced chemiluminescence, images were collected, and signal intensities were quantified using Eastman Kodak Co. Image Station 4000R.

### CYP2E1 activity assay

Activity of CYP2E1 was determined by measuring p-nitrophenol hydroxylation in whole liver extract as described earlier (Wu and Cederbaum, 2008).

## Isolation of RNA and quantitative real-time polymerase chain reaction (qRT-PCR)

Total RNA was isolated and reverse transcribed followed by amplification using qRT-PCR. The relative amount of target mRNA was determined using the comparative threshold (Ct) method by normalizing target mRNA Ct values to those of 18S (Mandal et al., 2010). The reaction mix (25  $\mu$ l) contained: cDNA, Applied Biosystems SYBR green kit (Life Technologies, Carlsbad, CA) and primers at final concentrations of 200  $\mu$ M. RT-PCR was performed in the Mx3000P cycler (Agilent, Santa Clara, CA): 95 °C for 10 min, 40 cycles of 15 s at 95 °C, 30 s at 60 °C, 30 s at 72 °C followed by 1 min at 95 °C, 30 s at 55 °C and 30 s at 95 °C. The relative amount of target mRNA was estimated using the comparative threshold (Ct) method by normalizing target mRNA Ct values to those of 18S (Mandal et al., 2010). Ct values were used for the statistical analysis of RT-PCR data.

## Immunohistochemistry

Formalin-fixed paraffin-embedded liver sections were de-paraffinized and stained for pimonidazole-adduct, Sirius red,  $\alpha$ -smooth muscle actin and cytokeratin-18 fragments/M30 staining. Frozen liver sections were used for staining HIF1 $\alpha$ , collagen 1 and Ly6c (Roychowdhury et al., 2012). All images presented in the results are representative of at least 3 images per liver and 4 mice per experimental condition.

## Statistical analysis

All values presented represent means  $\pm$  standard error of mean, with n=3–6 experimental points. Data were analyzed by ANOVA using the general linear models procedure (SAS, Carey, NC). Data were log transformed if needed to obtain a normal distribution. Follow-up comparisons were made by least square means testing. Student's t-test was used for comparing values obtained from two groups (used only for Figure 1).

## Results

### Moderate ethanol feeding induced hypoxia in mouse liver

Chronic ethanol feeding induces hypoxia in mouse liver (Nishiyama et al., 2012; Chiang et al., 2013). Using immunohistochemical staining, accumulation of hypoxia-sensing pimonidazole (PMD)-adducts was detected in mouse liver as early as 4 days after moderate ethanol feeding (4d, 11%, Figure 1A). PMD adducts were primarily visualized in hepatocytes around the central veins (Figure 1A). Moderate ethanol feeding for 4 days also increased HIF1 $\alpha$  protein expression in mouse liver (4d, 11%, Figure 1B), primarily localized around the central veins. HIF1 $\alpha$  protein accumulation was not detected in livers of HepHIF1 $\alpha$ -/- mice (Supplemental figure 1A).

Moderate ethanol feeding combined with CCl<sub>4</sub> exposure also increased HIF1 $\alpha$  protein accumulation in liver of wild-type, but not HepHIF1 $\alpha$ -/- mice (Supplemental figure 1B). HIF1 $\alpha$  protein accumulated in both the nucleus and cytosol and did not exhibit any zonal distribution.

## Hepatocyte-HIF1 $\alpha$ -deficiency reduced the numbers of apoptotic hepatocytes in mouse liver

Hepatocyte apoptosis is an important contributor to the progression of hepatic fibrosis (Canbay et al., 2004; Roychowdhury et al., 2012). Hypoxia induces apoptosis in a variety of cell types, including hepatocytes. Caspase-mediated cytokeratin-18 fragmentation, detected by M30 staining, is a specific indicator of hepatocyte apoptosis. While higher doses of ethanol induces hepatocytes apoptosis, moderate ethanol feeding alone does not result in hepatocyte apoptosis (Cohen et al., 2010). In contrast, CCl<sub>4</sub> exposure resulted in a modest degree of hepatocyte apoptosis, as detected by M30-positive hepatocytes. This response was exacerbated by concomitant ethanol feeding (Figure 2A/B). While hepatocyte-specific deletion of HIF1 $\alpha$  had no effect on M30-positive hepatocytes in pair-fed mice, the absence of HIF1 $\alpha$  in hepatocytes ameliorated the exacerbation of M30-positive hepatocytes in ethanol-fed mice (Figure 2A/B).

CYP2E1 expression, assessed by Western blot and enzymatic activity (Supplemental Figure 2), the concentration of ALT in the plasma and triglycerides in the liver were not affected by diet or genotype (Supplementary Table 1).

## Deficiency of HIF1 $\alpha$ in hepatocytes reduced acetyl-p53<sup>K386</sup> and PUMA expression in hepatocytes

In response to hypoxia, HIF1 $\alpha$  induces apoptosis in a p53-dependent manner (Sermeus and Michiels, 2011). p53 activity is regulated via both transcriptional and post-translational mechanisms. In particular, acetylation of p53 is essential for its activation and DNA-binding activity (Tang et al., 2008). Under the conditions of our study, neither CCl<sub>4</sub> exposure or ethanol feeding affected expression of p53 mRNA in the liver (data not shown). In contrast, the immunoreactive quantity of acetylated p53 (Ac-p53<sup>K386</sup>) was increased in response to CCl<sub>4</sub> exposure (Figure 3A). Further, concomitant ethanol feeding increased the numbers of Ac-p53<sup>K386</sup>-stained cells (Figure 3A, inset). Co-staining with Ac-p53<sup>K386</sup> and collagen 1 revealed that, while a major population of Ac-p53<sup>K386</sup> positive cells were localized in close proximity of the fibrotic septa, some of the Ac-p53<sup>K386</sup> positive cells were also visualized farther from the collagen fibers (Figure 3B). Deletion of HIF1 $\alpha$  in hepatocytes reduced the numbers of Ac-p53<sup>K386</sup>-positive cells following ethanol/CCl<sub>4</sub> exposure (Figure 3A).

PUMA, a p53-transcription-dependent effector molecule, is critical for p53-driven pro-apoptotic activities (Tang et al., 2008). PUMA expression was detected in both hepatocytes and NPCs in livers of CCl<sub>4</sub>-exposed mice, with higher numbers observed after ethanol feeding (Figure 3B). Hepatocyte-specific HIF1 $\alpha$ -deficiency reduced the numbers of PUMA-positive cells following ethanol/CCl<sub>4</sub> exposure (Figure 3C). However, the number of PUMA-positive cells following CCl<sub>4</sub> exposure in pair-fed mice was not different between livers of HepHIF1 $\alpha$ -/- compared to wild-type mice (Figure 3D).

## Hepatocyte-specific deletion of HIF1 $\alpha$ attenuated CCl<sub>4</sub>-induced fibrosis in mouse liver

Apoptosis is critical for progression of fibrosis in mouse liver. Since apoptosis of hepatocytes following moderate ethanol/CCl<sub>4</sub> exposure was HIF1 $\alpha$ -dependent, it would be expected to contribute in the exacerbation of fibrosis by ethanol. Moderate ethanol feeding

(11% of Kcal) during CCl<sub>4</sub> exposure increased liver fibrosis in C57BL/6 mice, resulting in enhanced bridging of Sirius red staining, compared to CCl<sub>4</sub>-treated pair-fed mice (Figure 4A/B). Like C57BL/6 mice, the parental HIF1 $\alpha$ <sup>fl/fl</sup> and Alb-cre mice also exhibited ethanol-driven increases in Sirius red staining following chronic CCl<sub>4</sub> exposure (Figure 4A/B).

If hepatocyte-HIF1 $\alpha$  contributes to ethanol-induced exacerbation of CCl<sub>4</sub>-mediated fibrosis, deficiency of HIF1 $\alpha$  in hepatocytes should ameliorate this increase of fibrosis. Hepatocyte-specific deletion of HIF1 $\alpha$  attenuated ethanol-induced exacerbation of CCl<sub>4</sub>-induced ECM deposition, as detected by Sirius red staining (Figure 4A/B). However, in pair-fed control mice, CCl<sub>4</sub>-induced hepatic ECM deposition was not influenced by the expression of HIF1 $\alpha$  in hepatocytes (Figure 4A/B).

Hepatic expression of collagen 1A1 mRNA (Figure 5C) and collagen 1 protein (Figure 5A/B) was also increased in the livers of C57BL/6 mice following combined exposure to ethanol and CCl<sub>4</sub>. Hepatocyte-specific HIF1 $\alpha$ -deletion attenuated the increase of CCl<sub>4</sub>-induced collagen 1A1 mRNA and collagen 1 protein expression in ethanol-fed mice but not in pair-fed control mice (Figure 5A/B/C).

Activation of HSC is a hallmark of liver fibrosis. In response to pro-fibrogenic stimuli, quiescent HSCs are transformed to their activated phenotype and produce collagen fibers in the liver. If hepatocyte-derived HIF1 $\alpha$  is involved in the activation of HSC during ethanol/CCl<sub>4</sub> exposure, then the HepHIF1 $\alpha$ <sup>-/-</sup> mice should be protected from this ethanol-induced amplification of HSC activation. Both mRNA (Figure 5F) and protein expression of  $\alpha$ SMA (Figure 5D/E), a marker of HSC activation, increased in the liver of C57BL/6 mice following combined exposure to ethanol and CCl<sub>4</sub> compared to mice pair-fed control-diets during CCl<sub>4</sub> treatment. Deletion of HIF1 $\alpha$  specifically in hepatocytes attenuated this ethanol-induced increase of  $\alpha$ SMA expression (Figure 5D/E/F).

### **HIF1 $\alpha$ -deficiency in hepatocytes reduced infiltration of monocytes/macrophages in mouse liver**

During early phases of liver fibrosis circulating innate immune cells, including Ly6c<sup>+</sup> monocyte/macrophages, migrate to the site of injury to engulf the damaged cells. If attenuation of fibrosis following ethanol/CCl<sub>4</sub>-combined exposure in the liver of

HepHIF1 $\alpha$ <sup>-/-</sup> mice was associated with reduced monocyte/macrophages infiltration, recruitment of Ly6c<sup>+</sup> cells to the liver should also be reduced in the livers of HepHIF1 $\alpha$ <sup>-/-</sup> mice. Ly6c<sup>+</sup> cells were increased following ethanol/CCl<sub>4</sub> combined exposure compared to CCl<sub>4</sub> in pair-fed control mice (Figure 6A/B). The majority of Ly6c<sup>+</sup> cells were localized in close vicinity of collagen fibers (Figure 6C). This increase in Ly6c<sup>+</sup> cells was reduced in CCl<sub>4</sub>-treated livers of ethanol-fed HepHIF1 $\alpha$ <sup>-/-</sup> mice compared to the C57BL/6 mice (Figure 6A/B). The number of Ly6c<sup>+</sup> cells was not different between HepHIF1 $\alpha$ <sup>-/-</sup> and wild-type pair-fed control mice exposed to CCl<sub>4</sub>.

## **Discussion**

Ethanol consumption induces hypoxia in the liver, particularly around the central veins (Nishiyama et al., 2012; Chiang et al., 2013). Hypoxia induces expression of multiple genes,



regulated by the hypoxia-sensing transcription factors, HIF1 $\alpha$  and HIF2 $\alpha$ , in a cell-type-dependent manner (Nath and Szabo, 2012). However, the contribution of hypoxia to development of ethanol-induced fibrosis has not yet been studied. Since chronic ethanol feeding, even at high ethanol concentrations, does not result in significant liver fibrosis in mice, we have recently adopted an alternative approach by exposing the mice to chronic CCl<sub>4</sub> in presence of a moderate ethanol-diet (Roychowdhury et al., 2012; Chiang et al., 2013). Using this model of ethanol-induced exacerbation of apoptosis and fibrosis, we have identified the importance of ethanol-induced hypoxia/HIF1 $\alpha$  signaling in mediating the response, associated with increased p53 acetylation, PUMA expression and hepatocyte apoptosis in livers from CCl<sub>4</sub>-exposed mice exposed to moderate ethanol. Importantly, hepatocyte-derived HIF1 $\alpha$  also contributed to ethanol-induced amplification of pro-fibrotic responses following chronic exposure to CCl<sub>4</sub>.

HIF1 $\alpha$ , an important mediator of cellular and systemic responses to hypoxia, regulates the expression of a variety of genes associated with different hepato-pathologies. Moderate ethanol exposure increased HIF1 $\alpha$  protein accumulation was detected in both nucleus and cytosol. Accumulation of HIF1 $\alpha$  in the cytosol could be a consequence of either a temporary saturation of the nuclear transport machinery for HIF1 $\alpha$  and/or a continued stabilization of HIF1 $\alpha$  prior to nuclear transport. Here we find that hepatocyte HIF1 $\alpha$  is an essential mediator of hepatocyte apoptosis in response to combined exposure to moderate ethanol and CCl<sub>4</sub>, but not in response to CCl<sub>4</sub> alone. Although, moderate ethanol exposure alone is insufficient to trigger apoptosis in hepatocytes, our data indicate that ethanol-induced HIF1 $\alpha$  accumulation acted to prime hepatocytes to a second injurious signal, e.g. CCl<sub>4</sub>, contributing to an exacerbated pro-apoptotic response.

This specific contribution of hepatocyte HIF1 $\alpha$  during moderate ethanol exposure is most likely a consequence of ethanol metabolism and the generation of a localized hypoxic environment. Metabolism of ethanol dysregulates energy metabolism, histone de-acetylation and apoptosis by impairing mitochondrial bioenergetics and NADH/NAD<sup>+</sup> ratio in hepatocytes (Zakhari, 2006). HIF1 $\alpha$  can also impair cellular redox balance by increasing glucose metabolism and reducing mitochondrial function (Vengellur et al., 2003). Therefore, it is likely that ethanol-induced hypoxia/HIF1 $\alpha$  expression sensitizes hepatocytes to a second hit, such as CCl<sub>4</sub>, leading to the increased pro-apoptotic environment in hepatocytes.

HIF1 $\alpha$ -driven apoptosis is largely p53-dependent (Sermeus and Michiels, 2011). While p53 expression is increased in some models of chronic ethanol feeding and CCl<sub>4</sub> exposure (Guo et al., 2013), post-translational modifications including acetylation, phosphorylation, methylation, sumoylation and ubiquitination mediate activation of p53 transcriptional activity. Phosphorylation prevents the binding of p53 with Mdm2, a negative regulator of p53 activation, while acetylation of p53 is central to its DNA-binding activity and upregulation of the downstream mediators, such as PUMA, NOXA and Bax, responsible for its pro-apoptotic activity (Tang et al., 2008). Recently, increased p53 acetylation has been implicated to hepatocyte apoptosis in a model of non-alcoholic fatty liver disease (Castro et al., 2013). Importantly, ethanol, both *in vivo* and in cultured cells, increases the acetylation of multiple proteins (Shepard and Tuma, 2009). The most well studied example is the ethanol-induced increase in histone acetylation that is mediated via decreased activity of

sirtuin 1 (SIRT1), an NAD<sup>+</sup>-dependent protein deacetylase (Zakhari, 2006). Increased NADH/NAD<sup>+</sup> ratios generated during ethanol metabolism serve to decrease the activity of SIRT1 in hepatocytes (Zakhari, 2006; Elliott and Jirousek, 2008). Here, we used immunoreactive Ac-p53<sup>K386</sup> as an indicator of p53 acetylation and detected increased Ac-p53<sup>K386</sup> in both hepatocytes and non-parenchymal cells near the fibrotic septa after CCl<sub>4</sub> exposure. Concomitant ethanol feeding and CCl<sub>4</sub> increased the numbers of Ac-p53<sup>K386</sup>-positive cells compared to pair-fed controls. Importantly, acetylation of p53 in response to ethanol and CCl<sub>4</sub> was HIF1 $\alpha$ -dependent. While we have not yet characterized the mechanism for increased acetylation of p53 under these conditions, it is known that acetylation of p53 is regulated via SIRT1-dependent deacetylation (Shepard and Tuma, 2009), consistent with a likely interaction between ethanol and SIRT1-dependent deacetylation in the context of ethanol and CCl<sub>4</sub>-induced injury.

As further evidence for an increase in p53-dependent transcriptional activity in response to ethanol/CCl<sub>4</sub>, expression of PUMA, a downstream target of p53 activation (Qiu et al., 2011) was also increased in a HIF1 $\alpha$ -dependent manner in hepatocytes and non-parenchymal cells. The reduction of PUMA-positive hepatocytes in livers of HepHIF1 $\alpha$ -/- mice is consistent with protection of hepatocytes from apoptosis in these mice.

Phagocytosis of dying hepatocytes induces a variety of pro-inflammatory cytokines/chemokines resulting in infiltration of monocytes and macrophages in the liver. Under the combined insult of moderate ethanol and CCl<sub>4</sub>, there was an increased recruitment of Ly6c<sup>+</sup> cell populations compared to mice treated with only CCl<sub>4</sub>. Deficiency of HIF1 $\alpha$  in hepatocytes reduced the numbers of hepatic Ly6c<sup>+</sup> cells following combined exposure to ethanol and CCl<sub>4</sub>. These data suggest that hepatocyte-derived HIF1 $\alpha$  contributes to increased hepatic infiltration of the pro-inflammatory/fibrotic populations of monocytes and macrophages following ethanol feeding, which in turn can modulate pro-fibrotic responses following exposure to CCl<sub>4</sub>. Reduced numbers of Ly6c<sup>+</sup> could be the result of altered chemokine release from HIF1 $\alpha$ -deficient hepatocytes and/or an indirect result of decreased HSC activation and fibrosis. The exact mechanistic interaction between HIF1 $\alpha$  in hepatocytes and the recruitment of Ly6c<sup>+</sup> cells from the circulation will require further investigation.

HIF1 $\alpha$  regulates the expression of a variety of genes associated with different hepatopathologies, including SREBP (Nishiyama et al., 2012), a critical mediator of ethanol-induced hepatic steatosis, as well as VEGF and iNOS, key genes for progression of liver fibrosis and angiogenesis (Keith et al., 2012). In response to hypoxia, hepatocytes also release a variety of pro-fibrotic molecules including PDGF-A, PDGF-B and plasminogen activator inhibitor (PAI-1) in a HIF1 $\alpha$ -dependent manner (Copple et al., 2009). Because ethanol metabolism results in a localized hypoxic environment within the liver, we hypothesized that HIF1 $\alpha$  in hepatocytes is critical for the amplification of fibrosis by even moderate concentrations of ethanol. Indeed, we find that HepHIF1 $\alpha$ -deficient mice are protected from the exacerbation of CCl<sub>4</sub>-induced fibrosis by moderate ethanol.

Interestingly, deficiency of hepatocyte-HIF1 $\alpha$  did not reduce the pro-fibrotic parameters in pair-fed mice exposed to CCl<sub>4</sub> alone, further indicating that hypoxia due to ethanol

metabolism may be a unique contributor to hepatic fibrosis in the context of CCl<sub>4</sub>. Induction of fibrosis in response to CCl<sub>4</sub>, a potent hepatotoxin, is initiated by hepato-cellular necrosis followed by a surge of hepatic inflammation. Moderate ethanol feeding has no direct impact on necrotic injury of hepatocytes by CCl<sub>4</sub>, as indicated by ALT concentrations in the plasma [14, supplemental table 1]. In turn the data suggest that increased apoptosis of hepatocytes during ethanol exposure drives increased activation of HSC and subsequent ECM production.

It is interesting to note that, in contrast to the hepatocyte HIF1 $\alpha$ -independent progression of fibrosis in control mice exposed to CCl<sub>4</sub>, liver fibrosis following bile duct ligation (BDL) is reduced in livers of HepHIF1 $\alpha$ <sup>-/-</sup> mice (Moon et al., 2009). The differential contribution of HIF1 $\alpha$  in BDL- versus CCl<sub>4</sub>-driven fibrosis could be a consequence of pathophysiological differences between these two models. In contrast to the hepatocyte apoptosis and necrosis induced by CCl<sub>4</sub>, development of fibrosis following BDL proceeds with less severe hepatocyte injury, instead triggered by increased portal inflammation and proliferation of biliary epithelia and oval cells (Starkel and Leclercq, 2011). Similarly, a differential role for PAI-1 in CCl<sub>4</sub> compared to BDL-induced fibrosis has been observed; PAI-1 is pro-fibrotic in CCl<sub>4</sub>-induced fibrosis, but anti-fibrotic during BDL-induced fibrosis (von Montfort et al., 2010).

In summary, we found that expression of HIF1 $\alpha$  in hepatocytes following moderate ethanol exposure is critical for amplification of CCl<sub>4</sub>-induced pro-apoptotic, as well as pro-fibrogenic, responses in mouse liver. Moreover, ethanol-induced fibrosis was associated with increased hepatic Ly6c<sup>+</sup> cells, suggesting that HIF1 $\alpha$  expression in hepatocytes also contributes to infiltration of monocyte/macrophage in the liver. Taken together, we have identified a critical link between activation of hepatocyte apoptosis, dependent on HIF1 $\alpha$ /p53 axis, and development of hepatic fibrosis using a mouse model of ethanol-induced liver fibrosis. The association between ethanol and increased acetylation of p53 is of potential clinical relevance, as a variety of drugs to enhance deacetylase activity are currently under investigation (Elliott and Jirousek, 2008; Shepard and Tuma, 2010).

## Supplementary Material

Refer to Web version on PubMed Central for supplementary material.

## Acknowledgments

*Financial support:* This work was supported in part by NIH grant RO1AA013868, P20 AA17069 and DOD #10248754 (LEN); American Liver Foundation fellowship (DJC); ABMRF/The Foundation for Alcohol Research (SR).

We are grateful to Dr. Colleen Croniger and Dave DeSantis for their help with the genotyping of HepHIF1 $\alpha$ <sup>-/-</sup> mice. The authors would also like to thank Manoa Hui for her assistance in preparing figure graphics, and to Jazmine Danner for her help in caring and breeding all animals used in this study.

## References

Battaller R, Brenner DA. Liver fibrosis. *The Journal of clinical investigation*. 2005; 115:209–218. [PubMed: 15690074]

- Bataller R, Rombouts K, Altamirano J, Marra F. Fibrosis in alcoholic and nonalcoholic steatohepatitis. *Best practice & research Clinical gastroenterology*. 2011; 25:231–244. [PubMed: 21497741]
- Canbay A, Friedman S, Gores GJ. Apoptosis: the nexus of liver injury and fibrosis. *Hepatology* (Baltimore, Md. 2004; 39:273–278.
- Castro RE, Ferreira DM, Afonso MB, Borralho PM, Machado MV, Cortez-Pinto H, Rodrigues CM. miR-34a/SIRT1/p53 is suppressed by ursodeoxycholic acid in the rat liver and activated by disease severity in human non-alcoholic fatty liver disease. *Journal of hepatology*. 2013; 58:119–125. [PubMed: 22902550]
- Chiang DJ, Roychowdhury S, Bush K, McMullen MR, Pisano S, Niese K, Olman MA, Pritchard MT, Nagy LE. Adenosine 2A Receptor Antagonist Prevented and Reversed Liver Fibrosis in a Mouse Model of Ethanol-Exacerbated Liver Fibrosis. *PloS one*. 2013; 8:e69114. [PubMed: 23874883]
- Cohen JI, Roychowdhury S, McMullen MR, Stavitsky AB, Nagy LE. Complement and alcoholic liver disease: role of C1q in the pathogenesis of ethanol-induced liver injury in mice. *Gastroenterology*. 2010; 139:664–674. 674 e661. [PubMed: 20416309]
- Copple BL, Bustamante JJ, Welch TP, Kim ND, Moon JO. Hypoxia-inducible factor-dependent production of profibrotic mediators by hypoxic hepatocytes. *Liver international : official journal of the International Association for the Study of the Liver*. 2009; 29:1010–1021. [PubMed: 19302442]
- Cursio R, Miele C, Filippa N, Van Obberghen E, Gugenheim J. Liver HIF-1 alpha induction precedes apoptosis following normothermic ischemia-reperfusion in rats. *Transplantation proceedings*. 2008; 40:2042–2045. [PubMed: 18675125]
- Ding WX, Ni HM, DiFrancesca D, Stolz DB, Yin XM. Bid-dependent generation of oxygen radicals promotes death receptor activation-induced apoptosis in murine hepatocytes. *Hepatology* (Baltimore, Md. 2004; 40:403–413.
- Dooley S, Hamzavi J, Ciuculan L, Godoy P, Ilkavets I, Ehnert S, Ueberham E, Gebhardt R, Kanzler S, Geier A, Breitkopf K, Weng H, Mertens PR. Hepatocyte-specific Smad7 expression attenuates TGF-beta-mediated fibrogenesis and protects against liver damage. *Gastroenterology*. 2008; 135:642–659. [PubMed: 18602923]
- Elliott PJ, Jirousek M. Sirtuins: novel targets for metabolic disease. *Current opinion in investigational drugs*. 2008; 9:371–378. [PubMed: 18393104]
- Greijer AE, van der Wall E. The role of hypoxia inducible factor 1 (HIF-1) in hypoxia induced apoptosis. *Journal of clinical pathology*. 2004; 57:1009–1014. [PubMed: 15452150]
- Guo XL, Liang B, Wang XW, Fan FG, Jin J, Lan R, Yang JH, Wang XC, Jin L, Cao Q. Glycyrrhizic acid attenuates CCl(4)-induced hepatocyte apoptosis in rats via a p53-mediated pathway. *World journal of gastroenterology : WJG*. 2013; 19:3781–3791. [PubMed: 23840116]
- Hirota SA, Beck PL, MacDonald JA. Targeting hypoxia-inducible factor-1 (HIF-1) signaling in therapeutics: implications for the treatment of inflammatory bowel disease. *Recent patents on inflammation & allergy drug discovery*. 2009; 3:1–16. [PubMed: 19149741]
- Keith B, Johnson RS, Simon MC. HIF1alpha and HIF2alpha: sibling rivalry in hypoxic tumour growth and progression. *Nature reviews Cancer*. 2012; 12:9–22.
- Mandal P, Roychowdhury S, Park PH, Pratt BT, Roger T, Nagy LE. Adiponectin and heme oxygenase-1 suppress TLR4/MyD88-independent signaling in rat Kupffer cells and in mice after chronic ethanol exposure. *Journal of immunology*. 2010; 185:4928–4937.
- Mehal WZ. HIF-1alpha is a major and complex player in alcohol induced liver diseases. *Journal of hepatology*. 2012; 56:311–312. [PubMed: 21963521]
- Moon JO, Welch TP, Gonzalez FJ, Copple BL. Reduced liver fibrosis in hypoxia-inducible factor-1alpha-deficient mice. *American journal of physiology*. 2009; 296:G582–592. [PubMed: 19136383]
- Mormone E, George J, Nieto N. Molecular pathogenesis of hepatic fibrosis and current therapeutic approaches. *Chemico-biological interactions*. 2011; 193:225–231. [PubMed: 21803030]
- Nath B, Szabo G. Hypoxia and hypoxia inducible factors: diverse roles in liver diseases. *Hepatology* (Baltimore, Md. 2012; 55:622–633.
- Nishiyama Y, Goda N, Kanai M, Niwa D, Osanai K, Yamamoto Y, Senoo-Matsuda N, Johnson RS, Miura S, Kabe Y, Suematsu M. HIF-1alpha induction suppresses excessive lipid accumulation in alcoholic fatty liver in mice. *Journal of hepatology*. 2012; 56:441–447. [PubMed: 21896344]

- Pritchard MT, Roychowdhury S, McMullen MR, Guo L, Arteel GE, Nagy LE. Early growth response-1 contributes to galactosamine/lipopolysaccharide-induced acute liver injury in mice. *American journal of physiology*. 2007; 293:G1124–1133. [PubMed: 17916644]
- Qiu W, Wang X, Leibowitz B, Yang W, Zhang L, Yu J. PUMA-mediated apoptosis drives chemical hepatocarcinogenesis in mice. *Hepatology* (Baltimore, Md. 2011; 54:1249–1258.
- Ramachandran P, Iredale JP. Liver fibrosis: a bidirectional model of fibrogenesis and resolution. *QJM : monthly journal of the Association of Physicians*. 2012a; 105:813–817. [PubMed: 22647759]
- Ramachandran P, Iredale JP. Macrophages: central regulators of hepatic fibrogenesis and fibrosis resolution. *Journal of hepatology*. 2012b; 56:1417–1419. [PubMed: 22314426]
- Rowe RG, Lin Y, Shimizu-Hirota R, Hanada S, Neilson EG, Greenson JK, Weiss SJ. Hepatocyte-derived Snail1 propagates liver fibrosis progression. *Molecular and cellular biology*. 2011; 31:2392–2403. [PubMed: 21482667]
- Roychowdhury S, Chiang DJ, Mandal P, McMullen MR, Liu X, Cohen JI, Pollard J, Feldstein AE, Nagy LE. Inhibition of apoptosis protects mice from ethanol-mediated acceleration of early markers of CCl<sub>4</sub>-induced fibrosis but not steatosis or inflammation. *Alcoholism, clinical and experimental research*. 2012; 36:1139–1147.
- Sermeus A, Michiels C. Reciprocal influence of the p53 and the hypoxic pathways. *Cell death & disease*. 2011; 2:e164. [PubMed: 21614094]
- Shepard BD, Tuma PL. Alcohol-induced protein hyperacetylation: mechanisms and consequences. *World journal of gastroenterology : WJG*. 2009; 15:1219–1230. [PubMed: 19291822]
- Shepard BD, Tuma PL. Alcohol-induced alterations of the hepatocyte cytoskeleton. *World journal of gastroenterology : WJG*. 2010; 16:1358–1365. [PubMed: 20238403]
- Starkel P, Leclercq IA. Animal models for the study of hepatic fibrosis. *Best practice & research Clinical gastroenterology*. 2011; 25:319–333. [PubMed: 21497748]
- Tang Y, Zhao W, Chen Y, Zhao Y, Gu W. Acetylation is indispensable for p53 activation. *Cell*. 2008; 133:612–626. [PubMed: 18485870]
- Vengellur A, Woods BG, Ryan HE, Johnson RS, LaPres JJ. Gene expression profiling of the hypoxia signaling pathway in hypoxia-inducible factor 1alpha null mouse embryonic fibroblasts. *Gene expression*. 2003; 11:181–197. [PubMed: 14686790]
- von Montfort C, Beier JI, Kaiser JP, Guo L, Joshi-Barve S, Pritchard MT, States JC, Arteel GE. PAI-1 plays a protective role in CCl<sub>4</sub>-induced hepatic fibrosis in mice: role of hepatocyte division. *American journal of physiology*. 2010; 298:G657–666. [PubMed: 20203062]
- Wang X, Wu D, Yang L, Gan L, Cederbaum AI. Cytochrome P450 2E1 potentiates ethanol induction of hypoxia and HIF-1alpha in vivo. *Free radical biology & medicine*. 2013; 63:175–186. [PubMed: 23669278]
- Wu D, Cederbaum A. Cytochrome P4502E1 sensitizes to tumor necrosis factor alpha-induced liver injury through activation of mitogen-activated protein kinases in mice. *Hepatology* (Baltimore, Md. 2008; 47:1005–1017.
- Wu YL, Piao DM, Han XH, Nan JX. Protective effects of salidroside against acetaminophen-induced toxicity in mice. *Biological & pharmaceutical bulletin*. 2008; 31:1523–1529. [PubMed: 18670083]
- Zakhari S. Overview: how is alcohol metabolized by the body? *Alcohol research & health : the journal of the National Institute on Alcohol Abuse and Alcoholism*. 2006; 29:245–254. [PubMed: 17718403]

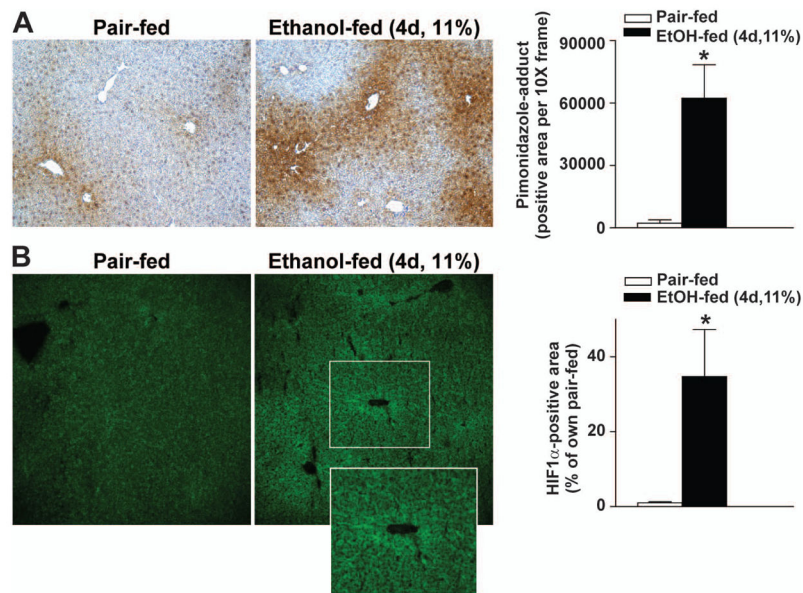


**Figure 1. Moderate ethanol feeding induced hypoxia and expression of HIF1 $\alpha$  in mouse livers** (A/B) C57BL/6J wild-type mice were allowed free access to ethanol-containing diets with (11% of kcal) or pair-fed controls. **(A)** Animals were injected with pimonidazole (PMD) 1 hour before euthanasia. Paraffin-embedded liver sections were de-paraffinized and stained for PMD-adducts. Images were acquired using 10X objective. **(B)** Frozen liver sections from pair- or ethanol-fed (11% of kcal) mice were stained for HIF1 $\alpha$ . Images were acquired using 20X objective. \*  $p < 0.05$  pair-fed compared to ethanol-fed mice.

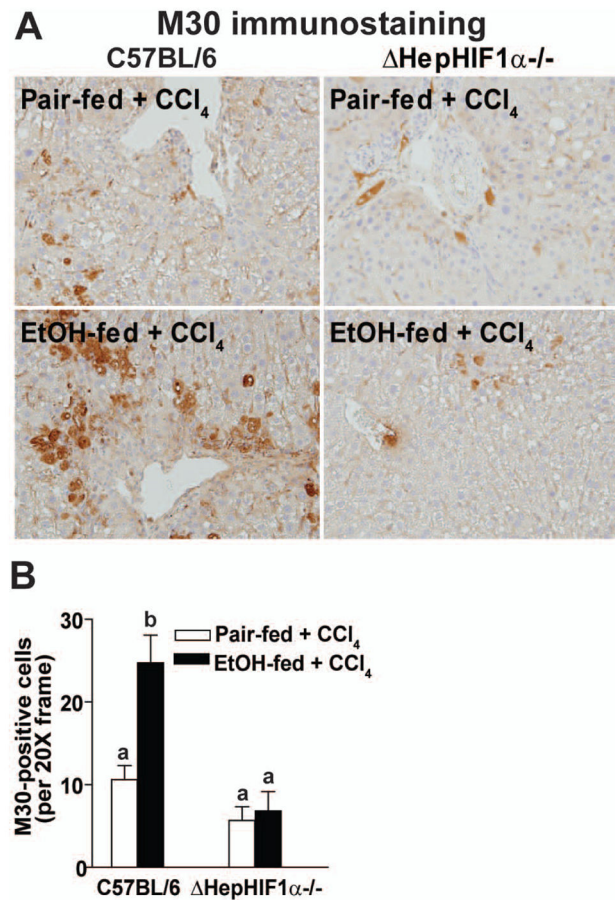


**Figure 2. Exacerbation of CCl<sub>4</sub>-induced hepatocyte apoptosis by ethanol was attenuated in livers of  $\Delta$ HepHIF1 $\alpha$ <sup>-/-</sup> mice**

C57BL/6 wild-type (WT) and  $\Delta$ HepHIF1 $\alpha$ <sup>-/-</sup> mice were allowed free access to diets with ethanol (11% of kcal) or pair-fed controls for 4 days followed by CCl<sub>4</sub> injections, as described earlier. (A) Paraffin-embedded liver sections were de-paraffinized and stained for M30/CK18 fragments, a marker for hepatocyte apoptosis. Images were acquired using a 20X objective. (B) Total numbers of M30<sup>+</sup> cells were counted. Values with different alphabetical superscripts were significantly different from each other,  $p < 0.05$ .  $n = 4-6$ .

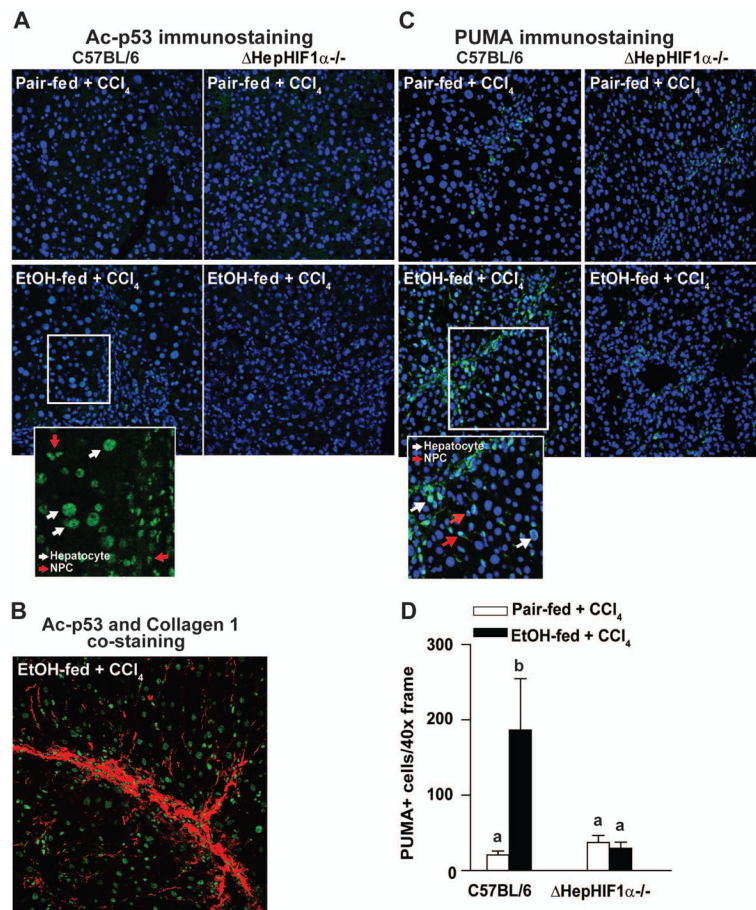


**Figure 3. Exacerbation of CCl<sub>4</sub>-induced p53 acetylation and PUMA expression by ethanol were attenuated in livers of HepHIF1 $\alpha$ -/- mice**

C57BL/6 wild-type (WT) and HepHIF1 $\alpha$ -/- mice were allowed free access to diets with ethanol (11% of kcal) or pair-fed controls for 4 days followed by CCl<sub>4</sub> injections, as described earlier. (A) Ac-p53<sup>K386</sup>, (B) Ac-p53<sup>K386</sup> (green) and collagen 1 (red) co-staining or (C) PUMA. Images were acquired using a 40X objective. PUMA (green) was co-stained with the nuclear stain DAPI (blue). (D) Total number of PUMA<sup>+</sup> cells was counted. Values with different alphabetical superscripts were significantly different from each other,  $p < 0.05$ .  $n = 4-6$ .



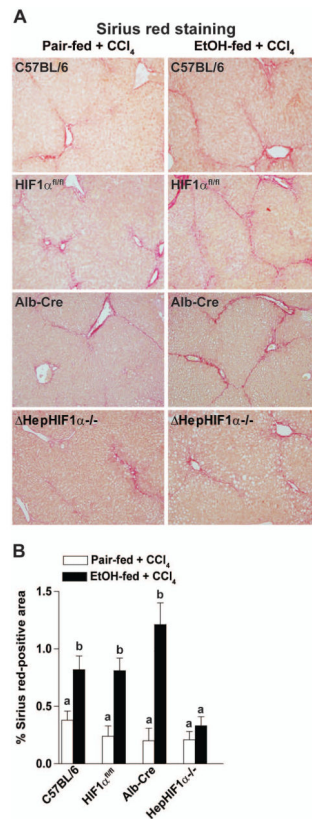


**Figure 4. Ethanol-induced exacerbation of CCl<sub>4</sub>-induced Sirius red staining was reduced in livers of HepHIF1 $\alpha^{-/-}$  mice**

C57BL/6, HIF1 $\alpha^{fl/fl}$ , Alb-cre and HepHIF1 $\alpha^{-/-}$  mice were allowed free access to diets with ethanol (11% of kcal) or pair-fed controls for 4 days followed by CCl<sub>4</sub> injections, as described in methods. (A) Paraffin-embedded liver sections were de-paraffinized and stained for Sirius red staining. Images are acquired using 20X objective. (B) Areas positive for Sirius red were quantified using Image Pro-Plus software and analyzed. Values with different alphabetical superscripts were significantly different from each other,  $p < 0.05$ .  $n=4-6$ .

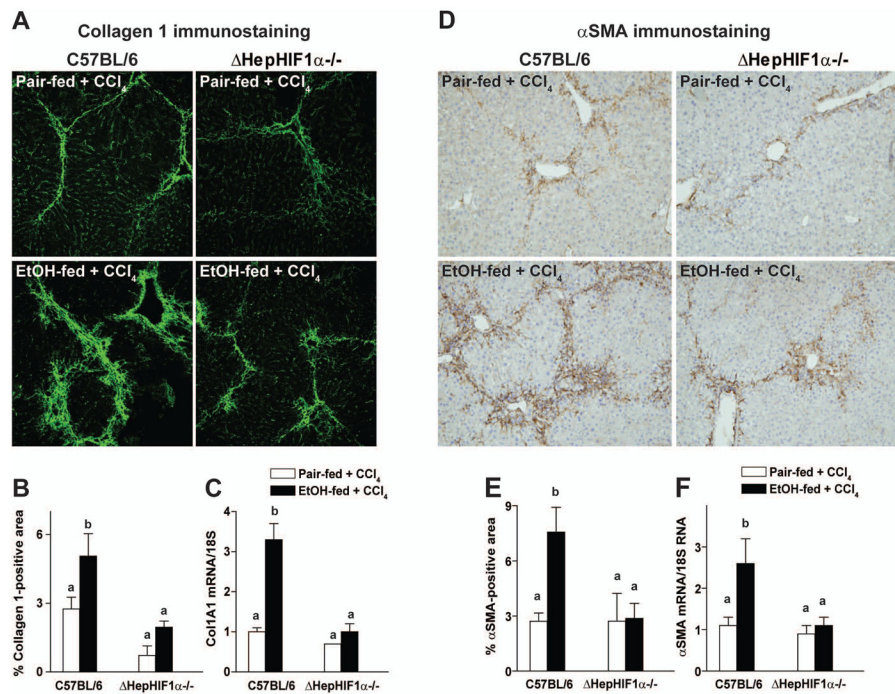


**Figure 5. Ethanol-induced exacerbation of CCl<sub>4</sub>-induced collagen 1 and smooth muscle actin expression were reduced in livers of HepHIF1α<sup>-/-</sup> mice**

C57BL/6 wild-type and HepHIF1α<sup>-/-</sup> mice were allowed free access to diets with ethanol (11% of kcal) or pair-fed controls for 4 days followed by CCl<sub>4</sub> injections, as described in methods. (A) Frozen liver sections were used for Collagen1 staining. Images are acquired using 20X objective. (B) Areas positive for collagen1 were quantified using Image Pro-Plus software and analyzed. (C) mRNA expression of Col1A1 was detected in mouse livers using qRT-PCR measurement. (D) Paraffin-embedded liver sections were de-paraffinized and stained for αSMA staining. Images are acquired using 10X objective. (E) Areas positive for αSMA were quantified using Image Pro-Plus software and analyzed. (F) mRNA expression of αSMA was detected in mouse livers using qRT-PCR measurement. Values with different alphabetical superscripts were significantly different from each other,  $p < 0.05$ .  $n = 4-6$ .

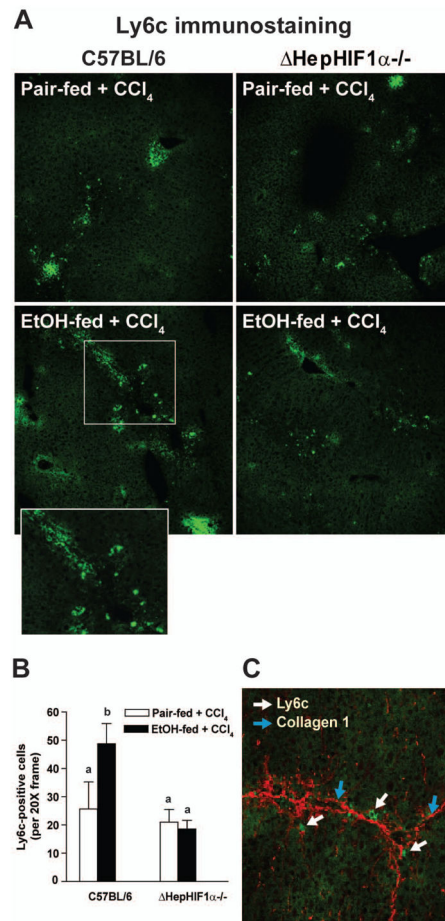


**Figure 6. Exacerbation of CCl<sub>4</sub>-induced Ly6c<sup>+</sup> cell infiltration by ethanol were attenuated in livers of HepHIF1 $\alpha^{-/-}$  mice**

C57BL/6 wild-type (WT) and HepHIF1 $\alpha^{-/-}$  mice were allowed free access to diets with ethanol (11% of kcal) or pair-fed controls for 4 days followed by CCl<sub>4</sub> injections, as described earlier. (A) Frozen liver sections were used for Ly6c staining. Images were acquired using a 20X objective. (B) Total numbers of Ly6c<sup>+</sup> cells were counted. Values with different alphabetical superscripts were significantly different from each other,  $p < 0.05$ .  $n = 4-6$ . (C) Ly6c<sup>+</sup> (green) and collagen1 (red) were co-stained in frozen liver sections from C57BL/6 mice exposed to both ethanol and CCl<sub>4</sub>. White arrows indicate collagen 1-stained fibers and blue arrows indicate Ly6c<sup>+</sup>-stained cells.